

# SURVEY TALK - NEW LASER AND OPTICAL RADIATION DIAGNOSTICS\*

W. P. Leemans

Center for Beam Physics, Accelerator and Fusion Research Division  
Ernest Orlando Lawrence Berkeley National Laboratory, Berkeley, CA 94720

## *Abstract*

New techniques are reported for electron beam monitoring, that rely either on the analysis of the properties of wiggler radiation (from static magnetic fields as well as from laser “undulators”, also referred to as Thomson scattering) or on the non-linear mixing of laser radiation with electron beam radiation. The different techniques reviewed are capable of providing information on femtosecond time scales and micron or even sub-micron spatial scales. The laser undulator is also proposed as a useful tool for non-destructive measurement of high power electron beams. An example is given of measuring electron beam energy and energy spread through spectral filtering of spontaneous wiggler radiation [1]. A novel technique based on fluctuational characteristics of radiation is described, for single shot, non-destructive measurement of the electron beam bunch length [2,3]. Thomson scattering based beam monitoring techniques are discussed which, through analysis of the radiated beam properties, allow non-destructive detailed measurement of transverse and longitudinal distributions of relativistic electron beams [4]. Two new techniques are discussed which rely on non-linear optical mixing of laser radiation with electron bunch emission: differential optical gating (DOG) [5] and electron bunch length measurement in a storage ring based on sum-frequency generation [6].

## 1 INTRODUCTION

Measurement of the transverse and longitudinal phase space properties of electron bunches produced in present and future high performance linacs [7-9], requires development of beam diagnostics with high spatial (micron or sub-micron) and temporal (femtosecond) resolution. Measurement of beam properties of high current, high power linacs [10] requires non-destructive diagnostics to be developed. Several diagnostics will be discussed, which rely on direct measurement of the properties of electron beam radiation, or on the interaction of that electron beam radiation with a laser beam. In each of the techniques discussed in this paper, the electron beam radiation is generated through interaction of the electron beam with static magnetic fields (e.g. wiggler radiation) or with electromagnetic radiation from a laser (Thomson scattering). Most of the techniques can be applied more generally to other types of radiation sources,

except when the unique property of a one-to-one correlation between observation angle and wavelength of the emission is used, such as in radiation originating from the interaction with magnetic fields.

Wiggler radiation (from permanent magnets, electromagnetic undulators and lasers) has been used for diagnostic purposes [1-3, 11-13] in a wide range of beam energies, as the radiation contains the full signature of the electron beam. In Section 2, a technique for measuring energy and energy spread through spectral filtering of spontaneous emission of a wiggler will be discussed [1] as well as a technique for bunch length monitoring through fluctuational interferometry of the incoherent light [2,3]. In Section 3, experiments using radiation from laser Thomson scattering [4] (i.e. electromagnetic undulator) for beam characterization will be reviewed. In Section 4, non-linear optical mixing of laser radiation with radiation from electron beams for longitudinal bunch profile measurements [5,6,14] will be discussed.

## 2 WIGGLER RADIATION

### *2.1 Beam Energy Diagnostic*

The wiggler emission cone contains information about the electron beam mean energy and energy spread [15,16]. A series of proof of principle experiments [1] have been carried out at the Accelerator Test Facility (ATF) at Brookhaven National Laboratory, demonstrating wiggler-based beam diagnosis in single shot mode, both for single micropulses and single macropulses. The experiments were performed using a high precision (0.08% peak amplitude rms) pulsed electromagnetic microwiggler from MIT, with a wiggler period of 8.8 mm. The high microwiggler field quality simplified the interpretation of the spectra defined by the convolution over many parameters: energy spread, divergence, spot size, matching, beam pointing and wiggler field errors. For a beam energy of 44-48 MeV, the wiggler emission was in the visible, where a wide range of optical diagnostics are available.

The wiggler emission profile was studied at the fundamental (532 nm). A narrow (1 nm) bandwidth interference filter was used to spectrally filter the radiation cones, and the full transverse far field pattern was recorded using a CCD camera. For a fixed wavelength, determined

---

\* Work supported by the US Department of Energy under contract No. AC03-76SF00098.

by the filter, the cone radius depends on beam energy and wiggler field strength, and the cone width contains information of divergence and energy spread. Analytic expressions were derived, showing that for energy spreads realistic for the linac (0.5% FW) at 48 MeV, divergence dominates over both energy spread and natural linewidth at sufficiently large angles [1]. For small cones, both effects are important. The far-field profile provides an advantage over the spectrum in divergence sensitivity. A systematic set of experiments was carried out to study cone response to beam energy, energy spread, wiggler field strength, electron beam misalignment and filter central wavelength. An electron beam divergence of 0.25 mrad was extracted in a single shot measurement. Examples of spontaneous emission cones are shown in Figure 1. Note that with a wiggler length of 70 periods, sensitivity to as little as 0.5% change in central beam energy was demonstrated.

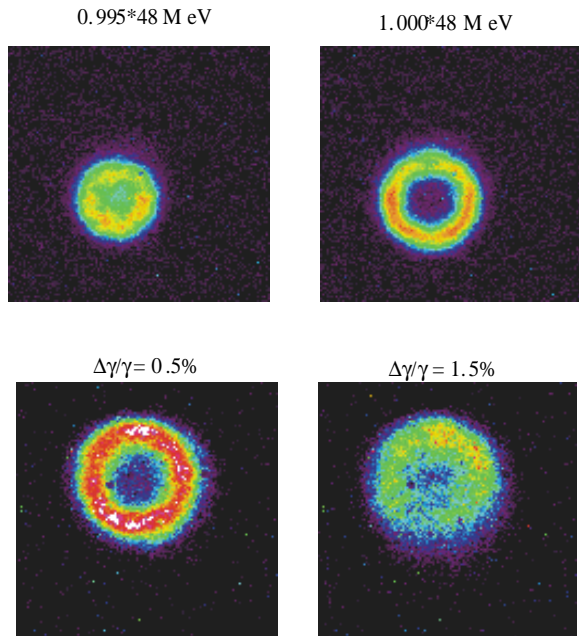


Figure 1. CCD images of a 1 nm portion of the far field wiggler spontaneous emission profile, showing sensitivity to beam energy (top pair – 48 MeV and 48\*0.995) and energy spread (bottom pair – 0.5% and 1.5% FW). From Ref. 1.

### 2.1 Fluctuational Interferometry

In 1995, a fluctuational interferometry technique relying on the incoherent contribution to the radiation was proposed [2]. For a radiation pulse to be longitudinally incoherent, the spectral bandwidth  $\Delta\omega$  must be much larger than the inverse of the pulse duration  $\tau_p$ , i.e.  $\Delta\omega\tau_p \gg 1$ . Using a bandpass filter, centered around  $\omega_0$  and with spectral width  $\delta\omega$ , temporal coherence can be imposed with an associated coherence time  $\tau_{coh} \propto \delta\omega^{-1}$ , effectively breaking the pulse up in  $N$  independent portions where  $N = \tau_p / \tau_{coh}$ . From shot-to-shot, the intensity will vary on the order of  $1/\sqrt{N}$ . Measurement of the variance of the intensity fluctuations will then give a measure for  $N$  and hence  $\tau_p \approx N / \delta\omega$ .

A proof of principle experiment was carried out at the ATF, in which the single shot spontaneous emission spectrum of the MIT microwiggler, was studied for a range of bunch lengths (1-7 ps) [1,3]. The microwiggler provided high brightness visible wavelength emissions for an electron beam energy of 44 MeV. A typical measured spectrum is shown in Figure 2a, revealing nearly 100% modulation and the presence of random spikes of a characteristic width, from which a bunch length of 2 ps was extracted. For comparison, a simulation for a similar bunch length including the measured instrumental resolution is shown in Figure 2b. The important features of the experimental data, the characteristic spike width and the level of modulation, are reproduced by the theory. Quantitative agreement has also been obtained between bunch length extracted from fluctuations and independent calibrations of beam bunch length [3].

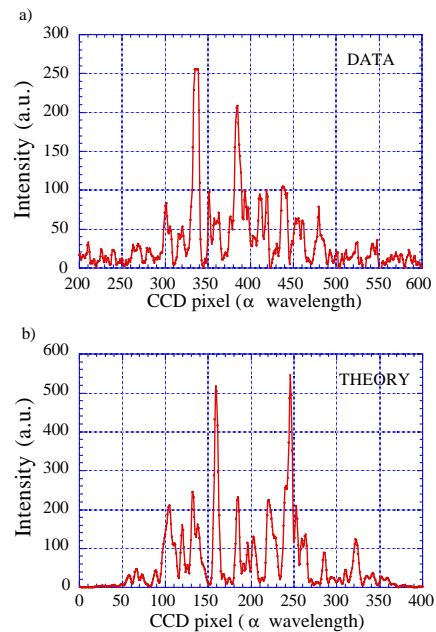


Figure 2. a) Single shot spontaneous emission spectrum from a microwiggler at 632 nm, showing nearly 100% modulation of the spectrum. Beam bunch length was extracted in a single shot measurement from the spectral fluctuations. b) A simulation for the same bunch length reproduces both the qualitative and quantitative features of the data.

## 3 LASER SCATTERING DIAGNOSTICS

A different approach to generating radiation from particle beams for beam monitoring is to use the interaction of the beam with high intensity laser fields. In effect, the laser acts as an electromagnetic undulator and the

properties of the emitted radiation can be accurately predicted using an equivalent undulator model [17]. The scattered radiation contains information on energy as well as on transverse and (for short laser pulses) longitudinal distributions of the electron beam.

At the Final Focus Test Beam (FFTB) at SLAC, transverse e-beam sizes as small as 70 nm were measured, by scanning a 50 GeV e-beam across the intensity fringes of an optical standing wave [7] produced by crossing two laser beams. The gamma ray yield depends on the number of photons with which the electron beam interacts and is therefore much larger at the peaks than at the valleys of the standing wave. Such resolution is beyond usual optical (e.g. optical transition radiation or synchrotron radiation) based methods.

A laser based beam diagnostic [4] which relies on analysis of the properties of the scattered radiation has been developed and used at the Beam Test Facility (BTF) [18] of the Center for Beam Physics at Lawrence Berkeley National Laboratory (LBNL). Some of the results of this experiment are discussed next.

### 3.1 Orthogonal Thomson Scattering Diagnostic

The experiment [4] was conducted at the BTF and used the 50 MeV ( $\gamma = 98$ ) linear accelerator (linac) injector of the Advanced Light Source in conjunction with a high power (40 mJ in 100 fs) short pulse laser system operating at 800 nm wavelength. Electron bunches were transported using bend magnets and quadrupoles to an interaction chamber where they were focused and scattered against the laser beam. After the interaction chamber, a  $60^\circ$  bend magnet deflected the electron beam onto a beam dump, away from the forward scattered x-rays. A 75 cm radius of curvature mirror was used to focus the S-polarized amplified laser pulses to about a  $30 \mu\text{m}$  diameter spot at the interaction point (IP) (measured by a charge coupled device (CCD) camera at an equivalent image plane outside the vacuum chamber).

To measure the spot size (and position) of the electron beam at the IP, an image of the electron beam was obtained by relaying optical transition radiation (OTR) [19] from a foil onto a 16 bit CCD camera or optical streak camera using a small f-number telescope. Electron beam spot sizes as small as  $35 \mu\text{m}$  rms have been measured.

During the interaction of an electron beam and laser beam, scattered x-ray photons are produced with energy  $U_x$ , given by (for  $\gamma \gg 1$ )

$$U_x = \frac{2\gamma^2 \hbar \omega_0}{1 + \gamma^2 \theta^2} (1 - \cos \psi), \quad (1)$$

where  $\omega_0$  is the frequency of the incident photons,  $\psi$  is the interaction angle between the electron and laser beam ( $\psi = \pi/2$  in our experiments), and  $\theta$  is the angle at which the radiation is observed and assumed to satisfy  $\theta \ll 1/\gamma$ . In the experiment, x-rays with a maximum energy of 30 keV (0.4 Å) are generated.

To measure the transverse electron beam distribution for a given slice of the electron beam, we scanned the laser beam transversely across the electron beam in steps of  $10 \mu\text{m}$ , by changing the tilt of the focusing mirror, and monitored the x-ray yield on the phosphor screen. It was found (Fig. 3) that the laser based technique and the results from OTR were in good agreement and give a half-width half maximum (HWHM) vertical size of  $66 \mu\text{m}$ . However, the measurements for the beam edges differed and were both non-Gaussian. From the OTR data an HWHM horizontal size of  $47 \mu\text{m}$  was obtained.

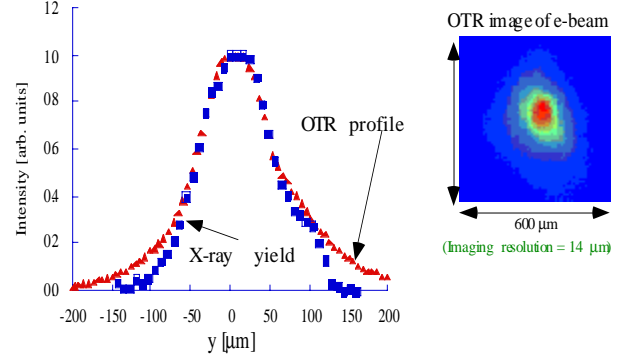


Figure 3: a) OTR image of the focused electron beam and b) triangle - vertical line-profile through the OTR image of the electron beam; square - x-ray yield vs. vertical laser beam position.

Measurement of the electron beam divergence for a fixed longitudinal location (i.e. fixed delay time between the laser and electron beam) of a time slice of the electron beam, with a duration equal to the convolution of the transit time of the laser pulse and the laser pulse duration, was done by monitoring the spatial x-ray beam profile on the phosphor screen using the CCD camera (see Fig.4). The scattered x-ray energy flux contains information of the angular distribution of the electron beam. By convoluting the single electron spectrum with a Gaussian distribution for the horizontal and vertical angles ( $\sigma_{\theta_x}$  and  $\sigma_{\theta_y}$  are the rms widths of the angular distribution of the electron beam in the horizontal and vertical direction respectively) and integrating over all energies and solid angle, the energy flux can be written as [4]:

$$\frac{dP}{d\theta_x d\theta_y} \propto \int_0^{2\pi} d\phi \int_0^1 d\kappa F(\kappa) \kappa [1 - 4\kappa(1-\kappa)\cos^2 \phi] \exp\left[-\frac{(\theta_x - \gamma^{-1} \sqrt{\frac{1}{\kappa} - 1} \cos \phi)^2}{2\sigma_{\theta_x}^2}\right] \exp\left[-\frac{(\theta_y + \gamma^{-1} \sqrt{\frac{1}{\kappa} - 1} \sin \phi)^2}{2\sigma_{\theta_y}^2}\right] \quad (2)$$

Here  $dP$  is the radiated x-rays intensity in a solid angle  $d\theta_x d\theta_y$ ,  $\phi$  is the azimuthal angle,  $F(\kappa)$  is an x-ray energy dependent function modeling the detector sensitivity and x-ray vacuum window transmission. Also,  $\kappa = U/U_{\max} = (1 + \gamma^2 \theta^2)^{-1}$  and  $U_{\max} = 2\gamma^2 \hbar \omega$  and a single incident laser frequency is assumed.

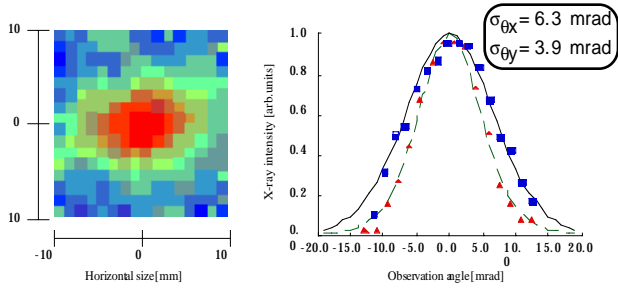


Figure 4. a) False color CCD image of the spatial profile of a 30 keV x-ray pulse on the phosphor screen, which is located 80 cm from the IP; b) square- horizontal line-profile and fitting curve (solid line), triangle -vertical line-profile and fitting curve (dashed line) from Fig. 4 (a). The scale has been converted into angular units.

By fitting the data (see Fig. 4) using Eq.(2), an electron beam divergence of  $\sigma_{\theta_x}$  ( $\sigma_{\theta_y}$ ) =  $6.3 \pm 0.2$  ( $3.9 \pm 0.2$ ) mrad was found.  $F(\kappa)$  was adjusted to account for the spectral dependence of the x-ray window transmission. The difference between  $\sigma_{\theta_x}$  and  $\sigma_{\theta_y}$  is due to a combination of the electron beam being focused astigmatically at the IP, resulting in a tilted phase space ellipse ( $y, y'$ ), and a laser spot size much smaller than the vertical electron beam size. As the laser beam crosses the focal volume of the electron beam, the complete horizontal (direction of propagation of the laser) phase space ( $x, x'$ ) is sampled by the laser beam. However, only electrons occupying the region in the vertical phase space defined by the spatial overlap with the laser beam will contribute to the x-ray flux. As opposed to the transition radiation based detector, the laser beam therefore acts as an optical microprobe of a finite region of the transverse phase space. This value of the electron beam divergence is also consistent with an effective angular divergence of the electron beam of 3.5 - 4 mrad obtained from analyzing the x-ray spectra. Of course, the main difference is that measurement of the spatial profile is a single shot technique as opposed to measuring the x-ray spectra which requires accumulation of thousands of shots.

Finally, since the x-ray yield is sensitive to both the longitudinal bunch profile and the degree of transverse overlap between the laser and electron beam, time-correlated phase space properties of the electron beam can be studied. When an electron bunch, which exhibits a finite time-correlated energy spread (chirp), is focused at the IP with a magnetic lattice which has large chromatic aberrations, different temporal slices of the bunch will be focused at different longitudinal locations. The transverse overlap between e-beam and laser will therefore strongly depend on which time slice the laser interacts with. This in turn will lead to a time dependence of the x-ray yield varying faster than the actual longitudinal charge distribution. To illustrate this, the x-ray flux was measured as a function of the delay between laser and e-beam, for two different magnetic transport lattices. In both lattices, the magnet settings were optimized to obtain a minimum electron beam spot size in the horizontal and vertical plane (as well as zero dispersion at

the IP), but chromatic aberrations were about 5 times larger in the second lattice. Result of a 60 ps long scan (time step of 1 ps) and time-resolved OTR from the streak camera for the lattice with low and high chromatic aberrations is shown in Fig. 5(a, b).

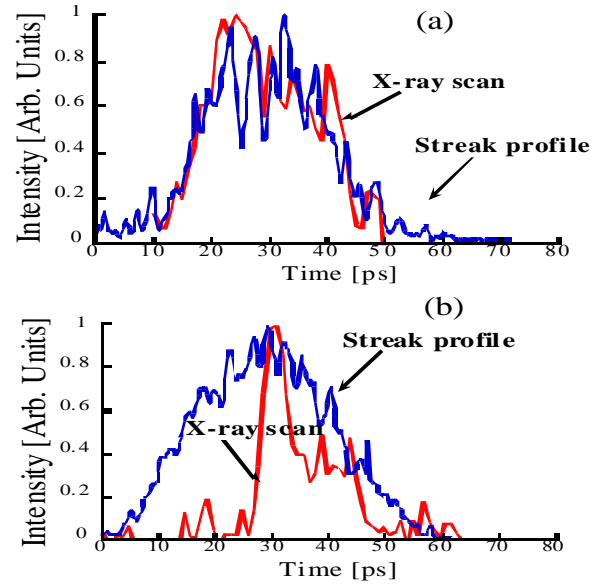


Figure 5: x-ray yield vs. delay time between laser and electron beam and profile of time resolved OTR image from a streak camera for a lattice with a) small and b) large chromatic aberrations.

Whereas the temporal scan for the lattice with low chromatic aberrations (Fig.5a) is in good agreement with the time-resolved OTR measured with a visible streak camera, the scans taken for the second configuration (Fig.5b) typically showed a 2-3 times larger amplitude 5 ps wide peak sitting on a 20 ps wide pedestal. This is to be compared to the time resolved OTR from the streak camera which typically showed a 25-30 ps wide electron beam without any sharp time structure. From lattice calculations, it is found that an energy change on the order of 0.25 % would increase the vertical spot size by a factor two at the IP, compared to best focus, resulting in a proportional reduction in vertical overlap between the laser and electron beam, and hence in x-ray yield. These measurements indicate the potential of the laser based Thomson diagnostic to measure time-correlated energy changes of less than a percent, with sub-picosecond time resolution.

It is important to note also that, due to the non-destructive nature of the Thomson scattering technique, it might prove to be a useful tool for the diagnosis of high current, high power electron beams, such as for the DAHRT project [10].

## 4 NON-LINEAR MIXING

Another new direction being pursued for developing beam diagnostics, is the non-linear mixing of laser radiation with radiation from electron beams [14]. Two recent

examples of the application of non-linear optics for bunch length monitoring are discussed next: one in which a tightly synchronized laser pulse is used to perform a cross-correlation measurement and one in which the laser pulse is loosely synchronized with respect to the electron beam.

#### 4.1 Laser Correlation with Synchrotron Pulses

Experiments at the Advanced Light Source have recently shown [6] that a synchronized laser pulse can be used to measure femtosecond synchrotron pulses via frequency up-conversion. Visible synchrotron radiation from the ALS at 2 eV was sum-frequency mixed in a BBO crystal with 1.55 eV radiation from a short pulse (<100 fs) Ti:Al<sub>2</sub>O<sub>3</sub> laser. By scanning the laser pulse in time with respect to the electron bunch, a 16.6 ps rms bunch length was measured, which is in good agreement with streak camera measurements. Furthermore, the technique was shown to detect sub-picosecond structure of the electron bunch, purposely imposed on the bunch by co-propagating an intense short laser pulse with the electron beam inside a wiggler. The laser beam, in the presence of a wiggler field, causes an energy modulation of a slice of the bunch via a FEL-like interaction. The energy modulation depth is determined by the wiggler and the laser pulse strength, and the duration of the slice is equal to the laser pulse length. By propagating the modulated electron beam through a dispersive section, this short slice can be separated from the main bunch, leaving a small density depression in the main bunch. The cross-correlation technique detected this few 100 fs long depression [6].

#### 4.2 Differential Optical Gating

The second example relies on the use of a loosely-synchronized laser pulse as a gate in a non-linear medium for pulse length measurement in a technique which is called differential optical gating (DOG) [5]. DOG uses two non-linear media as gates and two detectors (A and B). The gate pulse and the electron beam radiation are optically split in two parts. The laser reaching gate B is delayed by a time  $\delta$  with respect to the one reaching gate A. Under the assumption that the gate pulse is much shorter than the radiation pulse (and an instantaneous gate response), the signal seen by each detector can be written as [5]

$$\begin{aligned} A(t_1) &\propto E_G I_S(t_1) \\ B(t_1 + \delta) &\propto E_G I_S(t_1 + \delta) \end{aligned} \quad (3)$$

where  $E_G$  is the energy of the laser gate pulse and  $I_S(t)$  is the instantaneous intensity of the radiation. From this measurement, both the instantaneous intensity and its time derivative are then known, which allows bunch shape reconstruction. Through the loose synchronization, the laser pulse randomly “walks” across the bunch, much like interleaved sampling on digital oscilloscopes. In recent experiments at Stanford University, the technique

has been applied to the pulse shape measurement of a picosecond free electron laser source, using both an instantaneous gate and a step function gate [5].

## 5 ACKNOWLEDGEMENTS

I would like to thank Palma Catravas for kindly contributing to the section on the fluctuational interferometry and wiggler radiation measurements, R. Schoenlein and M. Zolotarev for information on the non-linear mixing, C. Rella and T. Smith for the DOG information, as well as my collaborators on the laser based probing work. I also want to thank E. Esarey for many useful conversations.

## 6 REFERENCES

- [1] P. Catravas, PhD thesis, MIT, 1998.
- [2] M. S. Zolotarev and G. V. Stupakov, SLAC-PUB-7132 (1995); M. S. Zolotarev and G. V. Stupakov, Proc. 1997 Particle Accelerator Conference.
- [3] P. Catravas et al., submitted to Phys. Rev. Lett.
- [4] W.P. Leemans et al., Phys. Rev. Lett. **77**, p.4182 (1996); R.W. Schoenlein et al., Science **274**, pp.236-238 (1996); W.P. Leemans et al., IEEE Journal of Quant. Elect. **33**, pp. 1925-1934 (1997).
- [5] C.W. Rella et al., submitted to Optics Comm.
- [6] R.W. Schoenlein, M. Zolotarev et al., private communication.
- [7] T. Shintake, Nucl. Inst. & Methods A**311**, pp. 453 (1992), Balakin, V. et al., Phys. Rev. Lett. **74**, p. 2479-82 (1995).
- [8] P. Kung, H. Lihn and H. Wiedemann, Phys. Rev. Lett. **73**, 967 (1994).
- [9] D. Umstadter et al., Phys. Rev. Lett. **76**, 2073 (1996); E. Esarey et al., Phys. Rev. Lett. **79**, 2682 (1997).
- [10] H. Rutkowski et al., these proceedings.
- [11] P. Heimann et al., Rev. Sci. Instrum., **66**(2) 1885-8 (1995).
- [12] A. Lumpkin, Nucl. Instr. & Meth. A, **393**, 170-177 (1997).
- [13] E. Tarazona and P. Elleaume, Rev. Sci. Instrum., **66**(2), 1974-7 (1995).
- [14] W.P. Leemans, Proc. Advanced Accelerator Concepts Workshop, AIP 398, Woodbury, NY (1997)
- [15] K.-J. Kim, AIP Conf. Proc. **184**, Vol.1, 565-632 (1989).
- [16] R. Barbini et al., Rivista del Nuovo Cimento, **13**(6), 1-65, (1990).
- [17] K.-J. Kim, S. Chattopadhyay and C.V. Shank, Nucl. Instr. And Meth. A **341**, 351-354 (1994).
- [18] W.P. Leemans et al., Proc. 1993 IEEE Part. Acc. Conf., 83, (IEEE, New York, 1993).
- [19] L. Wartski et al., J. Appl. Phys. **46**, 3644 (1975); M.J. de Loos, S.B. van der Geer and W.P. Leemans, Proc. EPAC 94, 1679 (1994).